

AperTO - Archivio Istituzionale Open Access dell'Università di Torino

**Redox-Driven Migration of Copper Ions in the Cu-CHA Zeolite as Shown by the In Situ PXRD/XANES Technique**

**This is the author's manuscript**

*Original Citation:*

*Availability:*

This version is available <http://hdl.handle.net/2318/1651664> since 2021-03-11T17:56:33Z

*Published version:*

DOI:10.1002/anie.201703808

*Terms of use:*

Open Access

Anyone can freely access the full text of works made available as "Open Access". Works made available under a Creative Commons license can be used according to the terms and conditions of said license. Use of all other works requires consent of the right holder (author or publisher) if not exempted from copyright protection by the applicable law.

(Article begins on next page)



# UNIVERSITÀ DEGLI STUDI DI TORINO

***This is an author version of the contribution published on:***

*Questa è la versione dell'autore dell'opera:*

*Angew. Chem. Int. Ed., 56, 2017, doi: 10.1002/anie.201703808*

***The definitive version is available at:***

*La versione definitiva è disponibile alla URL:*

*<http://onlinelibrary.wiley.com/doi/10.1002/anie.201703808/abstract>*

# Redox-Driven Migration of Copper Ions in the Cu-CHA Zeolite as Shown by the In Situ PXRD/XANES Technique

Casper Welzel Andersen<sup>1</sup>, Elisa Borfecchia<sup>2,3</sup>, Martin Bremholm<sup>1</sup>, Mads Ry Vogel Jørgensen<sup>1</sup>, Peter Nicolai Ravnborg Vennestrom<sup>2</sup>, Carlo Lamberti<sup>3,5</sup>, Lars Fahl Lundegaard<sup>2\*</sup>, and Bo Brummerstedt Iversen<sup>1\*</sup>

<sup>1</sup> Center for Materials Crystallography, iNANO, Department of Chemistry, Aarhus University, Langelandsgade 140, DK-8000 Aarhus, Denmark, E-mail: bo@chem.au.dk

<sup>2</sup> Haldor Topsøe A/S, Haldor Topsøes Allé 1, DK-2800 Kgs. Lyngby, Denmark, E-mail: lafl@topsoe.dk

<sup>3</sup> Department of Chemistry, NIS and CrisDI interdepartmental centers, University of Turin, Via P. Giuria 7, I-10125 Turin, Italy

<sup>4</sup> MAX IV Laboratory, Fotongatan 2, 225 92 Lund, Sweden

<sup>5</sup> IRC "Smart Materials", Southern Federal University, Zorge Street 5, RUS-344090 Rostov-on-Don, Russia

**Abstract:** Using quasi-simultaneous in situ PXRD and XANES we reveal the direct correlation between the oxidation state of Cu ions in the commercially relevant deNO<sub>x</sub> NH<sub>3</sub>-SCR zeolite catalyst Cu-CHA and the Cu ion migration in the zeolitic pores during catalytic activation experiments. A comparison with recent literature further reveals the high sensitivity of the redox-active centres concerning heating rates, temperature, and gas environment during catalytic activation. Previously, Cu<sup>+</sup> was confirmed present only in the 6R. Results verify a novel 8R monovalent Cu site, an eventually large Cu<sup>+</sup> presence upon heating to high temperatures in oxidative conditions, and demonstrate the unique potential in combining in situ PXRD and XANES techniques, with which we are able to track both oxidation state and structural location of the redox-active centres in the zeolite framework.

Concerning redox catalysts, whose active phase is deposited on an amorphous or highly disordered support, *e.g.* silica, carbons,  $\gamma$ -alumina, or similar, the understanding of the redox cycle can be achieved by *in situ* studies of the oxidation state of the active species by X-ray absorption near-edge spectroscopy (XANES).<sup>[1]</sup> When the active species is hosted in a crystalline matrix having different hosting sites, the situation becomes increasingly complex and a complete understanding may be reached only with an advanced experimental set-up allowing one to follow simultaneously long-range order changes *via* powder X-ray diffraction (PXRD) and the variation of the electronic state of the active species *via* XANES.

SSZ-13 (CHA) is an aluminosilicate zeolite with the chabazite structure.<sup>[2]</sup> It consists of double 6-rings and *cha*-cages, producing a small-pore three-dimensional network through 8-ring (8R) windows with an effective diameter around 3.8 Å at room temperature (RT).<sup>[3]</sup> Cu-loaded CHA (Cu-CHA) is currently applied as a catalyst for NH<sub>3</sub>-assisted selective catalytic reduction (NH<sub>3</sub>-SCR) of harmful nitrogen oxides (NO<sub>x</sub>), due to its enhanced activity, selectivity and hydrothermal stability compared to other medium- and large-pore zeolites.<sup>[4]</sup>

A detailed understanding of Cu speciation, location, and redox capability at elevated temperatures of Cu-CHA is a key step to unleash the potential of Cu-zeolite based deNO<sub>x</sub> catalysts. Several studies using diffraction techniques or X-ray absorption spectroscopy (XAS) have separately reported Cu sites and configurations in the 8R and 6R for Cu-CHA.<sup>[5]</sup>

High resolution PXRD analysed using Rietveld/maximum entropy method analysis has previously been used by Andersen *et al.*<sup>[5a]</sup> to report a complete structural model, represented in Figure 1, for dehydrated, O<sub>2</sub> activated Cu-CHA with similar composition as the present Cu-CHA sample (Si/Al = 15, Cu/Al = 0.45). The combined dehydration and O<sub>2</sub> activation was performed by slowly heating the sample in a capillary in air to 300 °C and maintaining the sample at elevated temperature for 1 h. Density functional theory (DFT) was used to determine the expected Cu species based on literature at the time, and the novel 8R site *B* was suggested to dominantly harbour 1Al[CuOH]<sup>+</sup> species, while the 6R sites harbour unligated 2AlCu<sup>2+</sup> ions (see Figure 2B).<sup>[5b,6]</sup> The complete structure includes three crystallographic Cu sites: two 6R sites, the central *A* and off-centered *A'* site and finally the novel 8R site *B*.

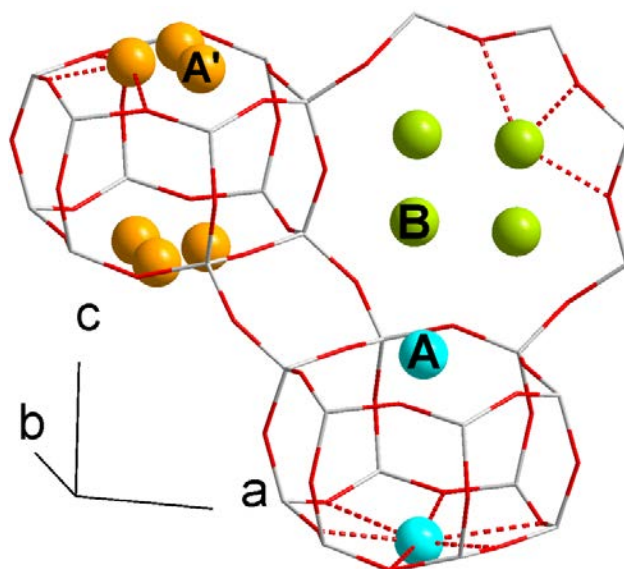


**Figure 1.** Crystallographic structure of dehydrated, O<sub>2</sub> activated Cu-CHA portraying the two 6R sites A (cyan) and A' (orange) and the 8R site B (green). Suggested bonds between Cu and framework O are shown with dashed lines. From Andersen *et al.*<sup>[5a]</sup>

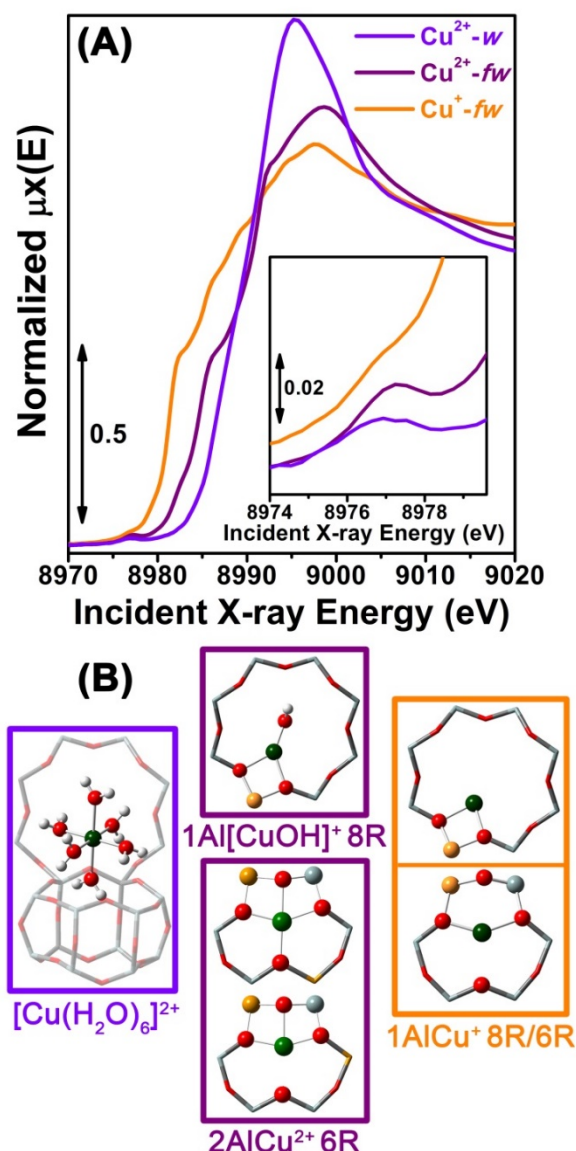
DFT-assisted XAS analysis previously allowed Borfecchia *et al.*<sup>[5b]</sup> to reveal different Cu species as a function of the dehydration temperature and gas feed in a Cu-CHA sample with composition equivalent to the one studied here. Whereas the catalyst at ambient conditions is dominated by mobile Cu<sup>2+</sup> aquo-complexes, activation in O<sub>2</sub> up to 400 °C yields the stabilization in the proximity of single Al sites of three-coordinated Cu<sup>2+</sup> species, bonded with two framework oxygens and one extra-framework OH<sup>-</sup> ligand. [CuOH]<sup>+</sup> complexes have been proposed also based on FTIR,<sup>[5b,6]</sup> although other Cu<sup>2+</sup>-oxo species, with similar coordination geometry and hence XANES signatures, could not be excluded to form, especially for temperatures above 400 °C. Conversely, activation in inert conditions (He flow) results in an almost complete reduction to Cu<sup>+</sup>, which previously has been connected to the loss of the OH<sup>-</sup> ligand in [CuOH]<sup>+</sup> species as the initial step.<sup>[5b,6-7]</sup> Figure 2A shows XANES spectra for these three key states of the Cu-CHA catalyst discussed and analysed in detail by Borfecchia *et al.* and employed here as reference for linear combination fit analysis (LCA). These include hydrated Cu<sup>2+</sup> (RT, air, labelled as Cu<sup>2+</sup>-w), framework-interacting Cu<sup>2+</sup> (O<sub>2</sub> activation at 400 °C, labelled as Cu<sup>2+</sup>-fw), and Cu<sup>+</sup> sites (He activation at 400 °C, labelled as Cu<sup>+</sup>-fw).

Figure 2B depicts DFT-optimized Cu geometries identified as the dominant structural component in each of the three experimental spectra, namely [Cu(H<sub>2</sub>O)<sub>n</sub>]<sup>2+</sup> or [Cu(H<sub>2</sub>O)<sub>n-1</sub>(OH)]<sup>+</sup> complexes ( $n = 5, 6$ , where only [Cu(H<sub>2</sub>O)<sub>6</sub>]<sup>2+</sup> is shown), 1Al[CuOH]<sup>+</sup>, and 1AlCu<sup>+</sup> sites. 2AlCu<sup>2+</sup> sites in 6R are also shown, representing a minor, reduction-resistant component expected to be present in a relative fraction < 20 % in both O<sub>2</sub> and He activated catalysts for the Si/Al ratio used herein.<sup>[5a,5b,7a]</sup>

Remarkably, XANES has played a key role in this assignment, due to its direct sensitivity to Cu oxidation state and local coordination geometry. It has been coupled with DFT-assisted fits in the extended X-ray absorption fine structure (EXAFS) region for the quantitative refinement of local environment of dominant Cu<sup>2+</sup> and Cu<sup>+</sup> species. However, due to the local character of the XAS techniques, it was difficult to reliably discriminate among similar coordination environments stabilized in the 6R or 8R of the CHA framework. With this respect, the combination with the long-range structural character of PXRD is expected to yield highly complementary insights.

It is well known that the NH<sub>3</sub>-SCR reaction includes a redox cycle of Cu, making the immediate understanding of Cu ion migration as a function of the oxidation state highly relevant and necessary.<sup>[8]</sup> To this end we employ time-resolved quasi-simultaneous PXRD and XANES *in situ* using synchrotron radiation,<sup>[9]</sup> exploiting the unique peculiarity of the BM01B (now BM31) beamline at ESRF. In short, a PXRD diffractogram is measured followed by the collection of four XANES spectra. This process takes ~5 min and is cyclically repeated while applying external heat to the sample. The Cu-CHA sample is confined in a capillary between two plugs of quartz wool, while

a dry stream of either 10 % O<sub>2</sub>/He or pure He is continuously flowing over the sample at 10 mL min<sup>-1</sup>. Further details can be found in SI.



**Figure 2.** (A) Reference Cu K-edge *in situ* XANES spectra of the Cu-CHA catalyst, representative of hydrated Cu<sup>2+</sup> (RT, air, labelled as Cu<sup>2+</sup>-*w*), and framework-interacting Cu<sup>2+</sup> (O<sub>2</sub> activation at 400 °C, labelled as Cu<sup>2+</sup>-*fw*) and Cu<sup>+</sup> sites (He activation at 400 °C, labelled as Cu<sup>+</sup>-*fw*); the inset shows a magnification of the pre-edge peak at 8977 eV mostly deriving from the dipole-forbidden Cu<sup>2+</sup> 1s→3d transition. (B) DFT-optimized Cu geometries identified as dominant and minor structural components for each catalyst state, namely Cu<sup>2+</sup> aquo-complexes, 1Al[CuOH]<sup>+</sup>, and unligated sites, 2AlCu<sup>2+</sup> and 1AlCu<sup>+</sup>. Atom colour code is as follows: Cu, green; H, white; O, red; Si, grey; Al, yellow. From Borfecchia *et al.*<sup>[5b]</sup>

In one part of the NH<sub>3</sub>-SCR reaction cycle Cu has oxidation state 2+.<sup>[8]</sup> A way of accessing this state is by activation in O<sub>2</sub> flow up to 500 °C.<sup>[10]</sup> Figure 3 summarizes the results obtained by following this activation *in situ* by quasi-simultaneous PXRD and XANES. Figure 3A shows the amount of Rietveld refined Cu ions per unit cell (Cu/uc) and water molecules per unit cell (Ow/uc), where water molecules are refined as oxygen atoms. In Figure 3B, another model has been used to analyse the PXRD data, where the total amount of Cu has been constrained to the value of 1.08 Cu/uc obtained by elemental analysis (see SI). It follows that Cu amounts here are shown as relative fractions. Due to a lower resolution in the current *in situ* PXRD data, simplified models using only the A and B sites (see Figure 1) have been applied in the Rietveld analyses. Further crystallographic details can be found

in SI. Figure 3C reports the relative fractions of the reference Cu K-edge XANES spectra (representative of hydrated  $\text{Cu}^{2+}$  ions, and framework interacting  $\text{Cu}^{2+}$  and  $\text{Cu}^+$  sites, see Figure 2) derived from LCA. Further details on LCA, corresponding R-factor values for each fit, etc., can be found in SI. Noteworthy, LCA of *operando* XANES data has recently allowed Lomachenko *et al.*<sup>[11]</sup> to track Cu-speciation in a Cu-CHA catalyst during  $\text{NH}_3$ -SCR in the 150–400 °C range, demonstrating the high sensitivity of the method once a reliable set of well-interpreted reference spectra is available.

From Figure 3 the sample starts out in a hydrated state, which is confirmed by both techniques. Mobile  $\text{Cu}^{2+}$ -aquo complexes present in hydrated Cu-CHA pores dominate the extra-framework electron density, which is why the used structure models only describe the data reliably after 45 min (including the dataset at 45 min), when a temperature of ~375 °C is reached.

XANES LCA shows a large linear increase in  $\text{Cu}^{2+}$ -fw species on account of the  $\text{Cu}^{2+}$ -aqua species until 150 °C is reached, after ~15 min. Hereafter, the increase is slower, but still linear.

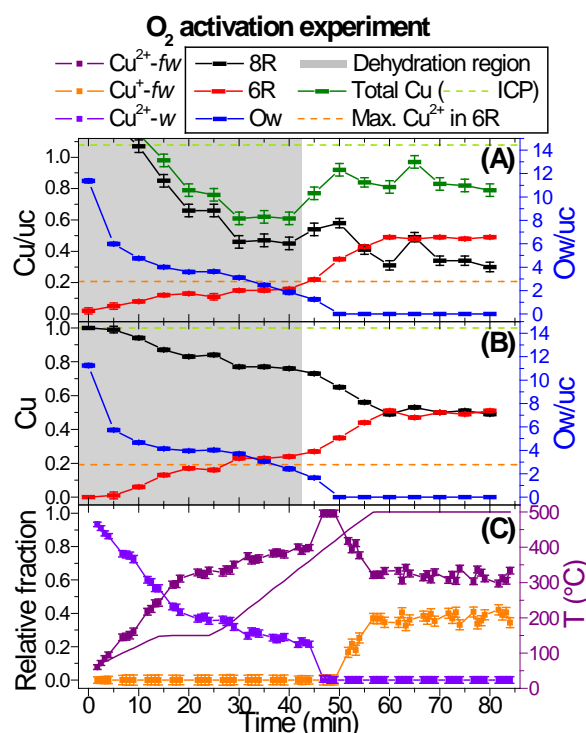


**Figure 3.** Analysis of the  $\text{O}_2$  activation of Cu-CHA from PXRD, without (A) and with (B) a total Cu constraint, and XANES (C). Boxed legend pertains to parts (A) and (B) containing information retrieved from Rietveld analyses of *in situ* PXRD data, while the non-boxed legend pertains to part (C) containing information retrieved from LCA of *in situ* XANES data. The registered average temperature is shown as a purple line in part (C). A plateau in the heating ramp at 150 °C was needed in order to change the heating rate from 6 °C  $\text{min}^{-1}$  to 10 °C  $\text{min}^{-1}$  until reaching the desired temperature of 500 °C. The “dehydration region” pertains to when the used structure model for Rietveld refinements does not reliably describe the data due to the influence of water. The catalyst is monitored for ~20 min after temperature stabilization at 500 °C in 10%  $\text{O}_2/\text{He}$  flow.

After ~48 min, when the sample is at ~400 °C,  $\text{Cu}^{2+}$ -w species are no longer detected by XANES. Their relative fraction decreases to 1(2) % and  $\text{Cu}^{2+}$ -w species are not present in the subsequent spectra. The PXRD data sets at 45 and 50 min, equivalent to ~375 and ~430 °C, respectively, show an equal loss of water from a refineable amount to a non-existent or rather non-refineable amount. This is an extraordinary example of the agreement between the two independent techniques and analysis methods, underlining the accuracy and applicability of their combination. Furthermore, the high temperature required for complete elimination of  $\text{Cu}^{2+}$ -w species suggests that the final water leaving must have been coordinated to Cu.

It is worth reminding that Bates *et al.*<sup>[12]</sup> reported a theoretical maximum limit of Cu<sup>2+</sup> ions in the 6R (exclusively as 2AlCu<sup>2+</sup> sites) based on statistical calculations and DFT calculations for Si/Al-ratios in the 2–47 range. For Si/Al = 15, the theoretical maximum for Cu occupancy in 2AlCu<sup>2+</sup> sites in the 6R corresponds to 0.21 Cu/uc and is shown as a dashed orange line in Figure 3A and B. By combining *in situ* spectroscopy and theoretical analysis, Paolucci *et al.*<sup>[7a]</sup> have recently identified such 2AlCu<sup>2+</sup> sites as the dominant structural component in O<sub>2</sub> activated Cu-CHA zeolites with Si/Al = 5, evidencing how these species are very difficult to reduce. Furthermore, their study confirms a very low abundance of these 2Al-sites in Cu-CHA catalysts with Si/Al = 15, where conversely the major Cu-species are redox-active 1Al[CuOH]<sup>+</sup> complexes.

This theoretical limit for Cu<sup>2+</sup> ions in the 6R is approximated by the occupancy plateau between 15 and 45 min, equivalent to the temperature range of ~150–375 °C (Figure 3A,B). Upon complete dehydration after ~48 min, LCA shows that all Cu is present as Cu<sup>2+</sup>-*fw* and for the constrained model, we achieve the same 8R/6R occupancy ratio as was seen by Andersen *et al.*<sup>[5a]</sup> In the following PXRD+XANES cycle, Rietveld analysis shows a significant increase of the 6R Cu occupation far above the theoretical limit for 2AlCu<sup>2+</sup> species, while LCA shows the progressive reduction of Cu<sup>2+</sup> into Cu<sup>+</sup>. The 6R Cu<sup>2+</sup> limit is exceeded for the remainder of the experiment. Simultaneously, PXRD shows a decrease in the 8R Cu occupancy, leading to the immediate conclusion that Cu<sup>2+</sup> in the 8R is the source for reduced Cu<sup>+</sup> in an oxidative atmosphere at high temperatures that is furthermore migrating to the 6R. This conclusion matches and directly confirms the reports that [CuOH]<sup>+</sup> species in the 8R are more easily reduced when compared to 2AlCu<sup>2+</sup> sites in the 6R.<sup>[5b,7a]</sup>

In the end, the 8R and 6R Cu occupancies are equal for the constrained model. However, the Cu<sup>2+</sup>/Cu<sup>+</sup>-ratio levels out around 60/40 = 1.5. This suggests that not all 8R Cu<sup>2+</sup> ions have reduced and migrated, or it may be that part of the 8R Cu species have only reduced, but not migrated, a situation mirroring that of the He activation experiment below. When the total Cu constraint is not applied to the Rietveld model, occupancy of the 6R tends to be slightly more favourable than the 8R, see Figure 3A. Also, the initial occupancy observed in the 8R is unchanged when the 6R occupancy increases significantly upon Cu reduction. This is due to an overall decrease of the refined total Cu occupancy, which may suggest an as yet unknown Cu site, perhaps in the vicinity of the 8R, but data with higher q-range are required to investigate this further. Since both models describe the data equally well (see SI), however, the migration of Cu from the 8R to 6R is unambiguous.

The migration from 8R to 6R during reduction from Cu<sup>2+</sup> to Cu<sup>+</sup> can be further monitored by activating the sample in an inert He flow up to 500 °C, which is known to yield a largely reduced Cu<sup>+</sup> state.<sup>[5b,6,13]</sup> Figure 4 shows the results of such activation performed with a heating rate of 10 °C min<sup>-1</sup> and followed with the same PXRD+XANES approach as described for the O<sub>2</sub> activation above.

As for the O<sub>2</sub> activation experiment, analysis of both PXRD and XANES data shows an initial hydrated state of Cu-CHA. The water removal from the framework was faster than in the O<sub>2</sub> activation. During the four XANES measurements between 20 and 27 min, when the temperature is between 310–378 °C, Cu<sup>2+</sup>-*w* species significantly decrease from a relative fraction of 0.13(1) to a negligible value of 0.013(20). The PXRD measurement at 25 min shows a remaining amount of water of 0.14(9) and 0.39(12) Ow/uc for the non-constrained and constrained models, respectively. In the subsequent PXRD and XANES measurements, no water or Cu-aquo complexes are detected.

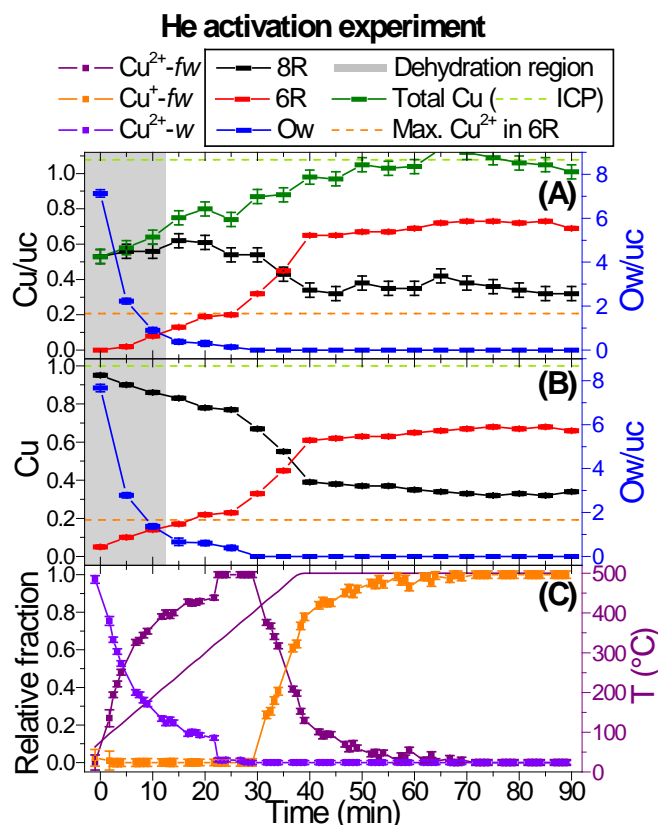


**Figure 4.** Analysis of the He activation of Cu-CHA from PXRD without (A) and with (B) a total Cu constraint and XANES (C). Boxed legend pertains to parts (A) and (B) containing information retrieved from Rietveld analyses of *in situ* PXRD data, while the non-boxed legend pertains to part (C) containing information retrieved from linear combination fits of *in situ* XANES data. The registered average temperature is shown as a purple line in part (C). The “dehydration region” pertains to when the used structure model for Rietveld refinements does not reliably describe the data due to the influence of water. The catalyst is monitored for ~50 min after temperature stabilization at 500 °C in He flow.

According to XANES LCA, while the water is slowly expelled from within the zeolite pores and cavities, the free floating  $\text{Cu}^{2+}$  aquo-complexes lose ligand water molecules and become  $\text{Cu}^{2+}\text{-fw}$  species, until only the latter are present in the zeolite from ~330–400 °C. At temperatures above 400 °C the XANES spectra show an initially rapid reduction of the  $\text{Cu}^{2+}$  species to  $\text{Cu}^+$  until a  $\text{Cu}^{2+}/\text{Cu}^+$ -ratio of 0.29(2) is reached. Then a slower reduction takes place, until all  $\text{Cu}^{2+}$  species are reduced to  $\text{Cu}^+$  after ~30 min at 500 °C. The change in reduction rates matches the point at which the temperature reaches and maintains 500 °C suggesting a thermally controlled redox-reaction. No further changes are observed in the analysis of the XANES spectra indicating equilibrium has been reached. Here it is worth to note that the relative fraction of  $\text{Cu}^+$  is slightly overestimated, since the Cu-CHA experimental spectrum employed as a reference for  $\text{Cu}^+\text{-fw}$  species also contains a minor contribution from non-reducible  $\text{Cu}^{2+}$  species (5–15 % of total Cu from previous study),<sup>[5b]</sup> most likely in the form of  $2\text{AlCu}^{2+}$  sites.

For the PXRD Rietveld refinements, data sets up to and including 10 min, equivalent to ~190 °C, are strongly influenced by the dominance of water in the electron density and therefore interpreted with great caution. As for the  $\text{O}_2$  activation experiment, the non-constrained model finds a decreased total amount of Cu, compared to the amount known to be present, and again the differences in agreement factors between the models are overall insignificant. However, this deficiency is only observed when Cu is present as  $\text{Cu}^{2+}$ . As the water amount decreases and temperature increases, the 6R is filling up to the theoretical maximum with  $2\text{AlCu}^{2+}$  species, and at ~310 °C after 20 min, the 6R occupancy levels out at this maximum. When XANES data begin to show a rapid reduction of Cu, after ~30 min, around 420 °C, PXRD data show an increase in the 6R Cu occupancy far above the theoretical  $\text{Cu}^{2+}$  limit. As when in oxidative conditions, the extra 6R Cu seems to originate from the 8R. However, due to the time resolution of our experiments (5 min per cycle) it is impossible to determine whether  $\text{Cu}^{2+}$  first migrate into the 6R, where they are reduced, or if they are first reduced in the 8R and then migrate to the 6R as  $\text{Cu}^+$  ions.



Furthermore, it seems a 6R occupancy limit is present for  $\text{Cu}^+$  as has been observed for  $\text{Cu}^{2+}$ , since the 6R Cu occupancy levels out around 0.70(3) Cu/uc upon reaching 500 °C for both models, while all Cu is still not completely represented by  $\text{Cu}^+$ -fw according to XANES LCA. The limit may arise from the Si/Al-ratio dependant amount of 6Rs containing 1 Al atom, or it may indeed be due to the small difference in energy associated with  $\text{Cu}^+$  residing in either site.

Through the combination of *in situ* PXRD and XANES measurements we can now directly show that  $\text{Cu}^+$  species are present in both the 6R and 8R simultaneously. Even though up to 15 % of the total Cu may be  $\text{Cu}^{2+}$  in the final 25 min of the experiment, producing a  $\text{Cu}^{2+}/\text{Cu}^+$ -ratio of 0.18, the 8R/6R-ratio far exceeds this, meaning the 8R must harbour  $\text{Cu}^+$  species. A plausible species-assignment for this novel  $\text{Cu}^+$  site in the 8R is given by the DFT-optimized structure, (reported in Figure 2B) previously proposed to form upon homolytic bond cleavage in  $1\text{Al}[\text{CuOH}]^+$  complexes.<sup>[5b]</sup>

Recently, Beale *et al.*<sup>[14]</sup> used *in situ* time-resolved PXRD to establish the Cu ion migration between 8R and 6R of Cu-CHA during an  $\text{O}_2$  activation and under active de $\text{NO}_x$  conditions. They showed upon heating Cu-CHA from RT to 500 °C in  $\text{O}_2$  that Cu migrates from the 8R to the 6R, almost depleting the 8R. Our study of Cu-CHA in an oxidative atmosphere does not show this effect to the same extent, however, a similar trend is observed. The differences may be due to the different Si/Al- and Al/Cu-ratios of the two investigated samples. In this study, the quasi-simultaneous acquisition of *in situ* XANES allows us to correlate Cu migration with partial reduction of the cations, observed also in  $\text{O}_2$  flow for temperatures higher than 400 °C. Overall, it emerges that the auto-reduction process in Cu-CHA, even at comparable catalyst composition, is strongly influenced by temperature, heating rate, and gaseous environment (e.g.  $\text{O}_2$  partial pressure) further emphasizing the necessity of advanced experimental set-ups simultaneously yielding structural and electronic state information on the active metal sites.

In conclusion, we have shown the power of combining *in situ* PXRD and XANES, when considering the intricacies of simultaneous cation migration and redox chemistry. Here we have used it to pinpoint a direct correlation between the reduction of Cu from  $\text{Cu}^{2+}$  to  $\text{Cu}^+$  and the migration of said species from an accessible, but relatively unstable configuration in the 8R of CHA to the less accessible, but more stable configuration in the 6R. Furthermore, the reduction process does not begin until all combinatory Cu-aquo species have split up, the water dissipated, and the kinetic energy overcomes a thermal activation energy corresponding to ~400 °C. Additionally, we have directly shown at least two separate  $\text{Cu}^+$  sites to be present in Cu-CHA, expanding the known  $\text{Cu}^+$ -loaded CHA model with an 8R site. Finally, we have shown that an  $\text{O}_2$  activation does not necessarily result in a Cu-CHA loaded only with  $\text{Cu}^{2+}$ , a  $\text{Cu}^{2+}/\text{Cu}^+$ -ratio around 1.5 is more reasonable with the experimental details used here, involving higher activation temperature (500 °C) and lower  $\text{O}_2$ -partial pressure with respect to our previous studies.<sup>[5a,5b]</sup> Thus when it comes to activation parameters and environment, the redox-active sites in the commercially relevant de $\text{NO}_x$   $\text{NH}_3$ -SCR catalyst Cu-CHA are fickle. Steadfast, when reduced in the 6R and predictable when using combined *in situ* PXRD and XANES analysis.

## Acknowledgements

This work was supported by the Danish National Research Foundation under the grant DNRF93, Center for Materials Crystallography (CMC). The Danish Agency for Science, Technology and Innovation (DANSCATT) is acknowledged for supporting the synchrotron activities. CL acknowledges mega-grant of Ministry of Education and Science of the Russian Federation (14.Y26.31.0001). EB acknowledges Innovation Fund Denmark (Industrial postdoc n. 5190-00018B). We thank Dr. W. van Beek for his competent help during beam time on BM01B (now BM31) at ESRF.

**Keywords:** Catalysis • Zeolites • X-ray diffraction • X-ray absorption spectroscopy • Structure-activity relationships

- [1] a) C. Lamberti, C. Prestipino, F. Bonino, L. Capello, S. Bordiga, G. Spoto, A. Zecchina, S. Diaz Moreno, B. Cremaschi, M. Garilli, A. Marsella, D. Carmello, S. Vidotto, G. Leofanti, *Angew. Chem. Int. Edit.* **2002**, *41*, 2341-2344; b) S. Bordiga, E. Groppo, G. Agostini, J. A. van Bokhoven, C. Lamberti, *Chem. Rev.* **2013**, *113*,

- 1736-1850; c) C. Paolucci, A. A. Verma, S. A. Bates, V. F. Kispersky, J. T. Miller, R. Gounder, W. N. Delgass, F. H. Ribeiro, W. F. Schneider, *Angew. Chem. Int. Edit.* **2014**, *53*, 11828-11833; d) J. H. Kwak, J. H. Lee, S. D. Burton, A. S. Lipton, C. H. F. Peden, J. Szanyi, *Angew. Chem. Int. Edit.* **2013**, *52*, 9985-9989.
- [2] a) S. I. Zones, **1985**, U. S. Patent 4,544,538; b) Z. Liu, T. Wakihara, K. Oshima, D. Nishioka, Y. Hotta, S. P. Elangovan, Y. Yanaba, T. Yoshikawa, W. Chaikittisilp, T. Matsuo, T. Takewaki, T. Okubo, *Angew. Chem. Int. Edit.* **2015**, *54*, 5683-5687.
- [3] C. Baerlocher, L. B. McCusker, "Database of Zeolite Structures", can be found under <http://www.iza-structure.org/databases/>, **2016**.
- [4] a) S. Brandenberger, O. Kröcher, A. Tissler, R. Althoff, *Catal. Rev.* **2008**, *50*, 492-531; b) J. H. Kwak, D. Tran, S. D. Burton, J. Szanyi, J. H. Lee, C. H. F. Peden, *J. Catal.* **2012**, *287*, 203-209.
- [5] a) C. W. Andersen, M. Bremholm, P. N. R. Vennestrom, A. B. Blichfeld, L. F. Lundegaard, B. B. Iversen, *IUCrJ* **2014**, *1*, 382-386; b) E. Borfecchia, K. A. Lomachenko, F. Giordanino, H. Falsig, P. Beato, A. V. Soldatov, S. Bordiga, C. Lamberti, *Chem. Sci.* **2015**, *6*, 548-563; c) A. M. Beale, F. Gao, I. Lezcano-Gonzalez, C. H. F. Peden, J. Szanyi, *Chem. Soc. Rev.* **2015**, *44*, 7371-7405; d) U. Deka, I. Lezcano-Gonzalez, B. M. Weckhuysen, A. M. Beale, *ACS Catal.* **2013**, *3*, 413-427; e) F. Göttl, P. Sautet, I. Hermans, *Angew. Chem. Int. Edit.* **2015**, *54*, 7799-7804.
- [6] F. Giordanino, P. N. R. Vennestrom, L. F. Lundegaard, F. N. Stappen, S. Mossin, P. Beato, S. Bordiga, C. Lamberti, *Dalton T.* **2013**, *42*, 12741-12761.
- [7] a) C. Paolucci, A. A. Parekh, I. Khurana, J. R. Di Iorio, H. Li, J. D. Albarracin Caballero, A. J. Shih, T. Anggara, W. N. Delgass, J. T. Miller, F. H. Ribeiro, R. Gounder, W. F. Schneider, *J. Am. Chem. Soc.* **2016**, *138*, 6028-6048; b) A. Godiksen, F. N. Stappen, P. N. R. Vennestrøm, F. Giordanino, S. B. Rasmussen, L. F. Lundegaard, S. Mossin, *J. Phys. Chem. C* **2014**, *118*, 23126-23138.
- [8] T. V. W. Janssens, H. Falsig, L. F. Lundegaard, P. N. R. Vennestrom, S. B. Rasmussen, P. G. Moses, F. Giordanino, E. Borfecchia, K. A. Lomachenko, C. Lamberti, S. Bordiga, A. Godiksen, S. Mossin, P. Beato, *ACS Catal.* **2015**, *5*, 2832-2845.
- [9] a) W. van Beek, O. V. Safonova, G. Wiker, H. Emerich, *Phase Transit.* **2011**, *84*, 726-732; b) J. Sottmann, F. L. M. Bernal, K. V. Yusenko, M. Herrmann, H. Emerich, D. S. Wragg, S. Margadonna, *Electrochim. Acta* **2016**, *200*, 305-313.
- [10] a) J. H. Kwak, R. G. Tonkyn, D. H. Kim, J. Szanyi, C. H. F. Peden, *J. Catal.* **2010**, *275*, 187-190; b) F. Gao, E. D. Walter, E. M. Karp, J. Luo, R. G. Tonkyn, J. H. Kwak, J. Szanyi, C. H. F. Peden, *J. Catal.* **2013**, *300*, 20-29.
- [11] K. A. Lomachenko, E. Borfecchia, C. Negri, G. Berlier, C. Lamberti, P. Beato, H. Falsig, S. Bordiga, *J. Am. Chem. Soc.* **2016**, *138*, 12025-12028.
- [12] S. A. Bates, A. A. Verma, C. Paolucci, A. A. Parekh, T. Anggara, A. Yezerets, W. F. Schneider, J. T. Miller, W. N. Delgass, F. H. Ribeiro, *J. Catal.* **2014**, *312*, 87-97.
- [13] a) G. T. Palomino, P. Fisicaro, S. Bordiga, A. Zecchina, E. Giamello, C. Lamberti, *J. Phys. Chem. B* **2000**, *104*, 4064-4073; b) S. C. Larsen, A. Aylor, A. T. Bell, J. A. Reimer, *J. Phys. Chem.* **1994**, *98*, 11533-11540.
- [14] A. M. Beale, I. Lezcano-Gonzalez, W. A. Slawinski, D. S. Wragg, *Chem. Commun.* **2016**, *52*, 6170-6173.